Biostability and biocompatibility of poly(ether)urethane containing gold or silver nanoparticles in a porcine model

Chih-Wei Chou,[1] Shan-hui Hsu,[1,2] Pey-Hwa Wang[3]
[1]*Department of Chemical Engineering, National Chung Hsing University, Taichung, Taiwan, Republic of China*
[2]*Institute of Biomedical Engineering, National Chung Hsing University, Taichung, Taiwan, Republic of China*
[3]*Department of Animal Science, National Taiwan University, Taipei, Taiwan, Republic of China*

Received 3 November 2006; revised 29 January 2007; accepted 31 January 2007
Published online 17 July 2007 in Wiley InterScience (www.interscience.wiley.com). DOI: 10.1002/jbm.a.31387

Abstract: Nanocomposites from polyether-type waterborne polyurethane (PU) incorporated with different amounts of gold nanoparticles (17.4–65 ppm) or silver nanoparticles (30.2–113 ppm) were prepared. Specifically, the nanocomposite containing 43.5 ppm of gold or 30.2 ppm of silver was previously found to possess the best thermal and mechanical properties. The enhanced biostability of the nanocomposite at the specific nanoparticle content was also observed in subcutaneous rats. The latter was probably related to the free radical scavenging ability of the nanocomposite shown *in vitro*. In this study, the *in vivo* biostability of the full series of these nanocomposites was assessed by porcine subcutaneous implantation for 19 days followed by microscopic examination and chemical characterization using attenuated total reflectance–infrared spectroscopy (ATR-IR). The nanocomposite at 43.5 ppm of gold ("PU-Au 43.5 ppm") and that at 30.2 ppm of silver ("PU-Ag 30.2 ppm") exhibited superior biostability in pigs to those at higher or lower nanoparticle contents. In particular, evidence of oxidative chain scission and crosslinking of the surface was presented by ATR-IR spectra in the explanted PU and nanocomposites other than PU-Au 43.5 ppm and PU-Ag 30.2 ppm. The extent of biodegradation and that of foreign body reactions were highly associated in these nanocomposites, both of which showing negative correlation with the free radical scavenging ability. The interdependency among antioxidation/biostability/biocompatibility of PU was demonstrated in this porcine model. © 2007 Wiley Periodicals, Inc. J Biomed Mater Res 84A: 785–794, 2008

Key words: polyurethane; nanocomposites; biostability; gold nanoparticles; silver nanoparticles

INTRODUCTION

Polyurethane (PU) elastomers have been extensively used in many biomedical devices for over 40 years because of their excellent biocompatibility and mechanical properties.[1,2] Recently, the development of waterborne PU formulations has dramatically increased because of the environmental demand.[3,4] The ether-type waterborne PU was unfortunately susceptible to oxidative biodegradation in a biological environment, similar to that occurred in the solvent-borne poly(ether)urethanes (PEU).[5–7] Highly reactive oxygen species produced by the macrophages and other phagocytes during inflammation may initiate the oxidation by free radical reactions. For this reason, solvent-borne PEU have been modified of the chemical structure[8–10] or added with antioxidants such as vitamin E, to improve their biostability.[11,12]

Correspondence to: S.-h. Hsu; e-mail: shhsu@nchu.edu.tw
Contract grant sponsors: National Science Council (Taiwan), National Health Research Institutes (Taiwan)

Several studies have been performed on the preparation of new polymer-metal nanocomposites.[13–16] The advantages of these nanocomposites can be much more remarkable than those observed in conventional composites because of the high surface to volume ratio of the metal nanoparticles. In our previous studies,[17–19] gold and silver nanoparticles were added to a waterborne PEU to improve their thermal and mechanical properties as well as biostability. The purpose was successfully achieved when a specific amount of gold (43.5 ppm) or silver (30.2 ppm) nanoparticles was used. The improved thermal and mechanical properties were related to the enhanced hydrogen-bonding between hard segments upon addition of Au or Ag nanoparticles.[17,19] In addition, the enhanced biocompatibility demonstrated *in vitro* was attributed to the surface nanofeatures and the free radical scavenging effect of the nanocomposites.[20] The free radical scavenging ability of the nanocomposites at the specific nanoparticle contents may also account for their biostability in rats.[18,19] In spite of the promising results, the *in vivo* data of biostability for these nanocomposites have not been fully established yet. For example, the biostability of the

nanocomposites not at the specific nanoparticle contents was not studied. The *in vivo* degraded samples were neither characterized properly. Consequently, there was lack of direct proof for the relations among antioxidation, biodegradation, and foreign body reactions in our system.

Schubert et al.[11,12] and others in the same research group[21,22] have investigated vitamin E or Santowhite as an antioxidant for the implanted PEU. It was demonstrated that the antioxidants prevented chemical degradation of PEU, and protected the PEU surface from severe pitting and cracking. This research group has hypothesized that a feedback system of cell-polymer interaction controlled the effect of the polymer on the host (biocompatibility) and the host on the polymer (biostability). Possible degradation products from scission of PEU soft-segments could act as "feedback" signals to foreign body giant cells (FBGCs) to modulate the behavior of adherent FBGCs. The advantage of the current nanocomposite system was that the variation in the oxidative stability of PU at different nanoparticle contents was not monotonous[20] (e.g. the addition of 43.5 ppm Au in PEU was best followed by 65 and 17.4 ppm), which allowed us to see tendency of change. Another advantage was that the small amount of nanoparticles used should not determine the chemical compositions. This avoided the contribution from chemical difference.

To confirm the interdependency of antioxidation, biostability, and biocompatibility in our PU nanocomposites, chemical characterization of the *in vivo* degraded samples[11] at different nanoparticle contents was necessary. Therefore, a series of polyurethane–gold (PU-Au) and polyurethane–silver (PU-Ag) nanocomposites were implanted in porcine subjects and the explanted samples were characterized by optical microscopy, SEM, and ATR-IR for a complete biostability study *in vivo*.

MATERIALS AND METHODS

Materials

Poly(tetramethylene glycol) (PTMO; 2000 g/mol), from Coating Chemical Industrial, Taiwan, was degassed at 70°C. Methylene dicyclohexane diisocyanate (H_{12}MDI) and EES-200L (N-(ethylene sulfonate sodium salt) ethylene diamine, 45% aqueous solution), from Jiuh Yi Chemical Industrial, Taiwan, as well as ethylene diamine and di-*n*-butyltin dilaurate, from TCI, were used as received. Acetone was distilled prior to reaction. The solution of gold nanoparticles and the solution of silver nanoparticles were supplied by Global Nanotech Industries, Taiwan. The solution was a dispersion of gold or silver fine particles in water (about 17.5 ppm/mL for Au or 27.2 ppm/mL for Ag). The diameters of the Au and Ag nanoparticles were both uniform and about 5 nm, which have been confirmed by transmission electron microscopy.[17,19]

Polyurethane synthesis

In this study, the waterborne PU was prepared from acetone process. The synthesis procedures of waterborne PU were described briefly as follows. PTMO (200 g) and stoichiometric H_{12}MDI (1:2) were charged into a four-neck kettle reaction equipped with nitrogen inlet, outlet, mechanical stir, and a thermometer. The reaction took place under nitrogen flow at 70°C and was monitored by dibutyl amine titration.[23] When the end-point of reaction had been reached, around 250 g of acetone was added into the reaction kettle, while the reaction mixture was cooled down to room temperature. This was followed by addition of EES-200L and stirring was continued for additional 30 min. Deionized water was introduced into the reaction mixture with vigorous stirring. After the addition of deionized water, ethylene diamine was added for further chain extension. Finally, acetone in the reaction mixture was removed by vacuum.

Preparation of PU-Au and PU-Ag nanocomposite films

PU-Au and PU-Ag nanocomposites films were prepared by adding a certain calculated volume of Au or Ag nanoparticle (containing 17.4–65 ppm of Au or 30.2–113 ppm of Ag in the final weight) into 10% solution of PU. The mixture was cast onto Teflon plates, dried at 60°C for 48 h, followed by further drying in a vacuum oven at 60°C for 72 h to remove any residual solvent. The films were stored in a desiccator at room temperature.

In vivo biostability by porcine implantation

The PU samples ($\sim$0.5 mm thick) were cut into 1 cm $\times$ 2.5 cm specimens, sterilized with 70% ethanol, rinsed, and placed in PBS. Biostability was assessed by subcutaneous implantation of the samples in the dorsal region of pigs. The pigs employed were small ear Lee-Sung strain experimental pigs in 5-month-old and in good health, weighing approximately 31–41 kg. Animals were anaesthetized with Zoletil 50 (0.1 mg/kg) and Atropine sulphate (1 mg/kg), followed by mask inhalation of 3% isoflurane. The hair on the back of the pigs was carefully clipped, on both sides of the spine ($\sim$30 cm $\times$ 5 cm). The areas were cleaned by 70% ethanol. On each side, four incisions with size approximately 1 cm $\times$ 3 cm were created by a surgical knife. Then the samples were inserted into the subcutaneous sites. The skin wounds were closed by Polysorb suture no.3 (Auto Suture, USA). Four pigs were used for each material. Nineteen days later, the pigs were anaesthetized and the implanted samples and surrounding tissues were taken out. Some of the samples were washed carefully with Triton X-100 to remove adherent cells. Then they were rinsed with distilled water and vacuum dried for viewing of surface biodegradation under a reflective optical microscope

(Nikon Labophot, Japan) or SEM described below, and for ATR-IR characterization. Surface roughening, cracking or pitting is a sign of oxidative biodegradation.[24–26] The other samples were fixed by formaldehyde, embedded, microtomed, and stained by H&E for histological analysis.

Scanning electron microscopy

A JEOL JSM-6700F field emission scanning electron microscope (FESEM) was used to collect a standard set of SEM images of explanted specimens and unimplanted reference samples at magnification up to 1000× for evidence of surface degradation. It was operated at a working distance of 11 mm, an acceleration voltage of 5 kV, and a beam current of 1×10^{-10} A. The dried specimens were made conductive with a 3-nm layer of gold using a Cressington Rotating Magnetron Sputter Coater operated at a working distance of 150 mm and a current of 20 mA. Each sample was ranked on a scale of 1 (no evidence of biodegradation, smooth surface) to 6 (extensive deep cracking of the entire surface) as described in the following guidelines: ranking of 1, specimen smooth on surface and no cracking observed; 2, patches of fine cracking or pitting over less than 10% of surface area; 3, patches of fine cracking or pitting over 10–70% of surface area; 4, fine cracking or pitting over greater than 70% of surface area; 5, any deep cracking covering less than 70% of surface area; 6, Deep cracking covering more than 70% of surface area and/or loss of materials.[27]

Attenuated total reflectance infrared spectroscopy

The surface chemical structure of all the samples (pure PU, PU-Au, and PU-Ag) before and after 19 days implantation was analyzed by attenuated total reflectance ATR-IR spectroscopy (Jasco 410, ATR PRO-410-S). The angle of incidence used was 45° and held constant for all measurements. About 40 scans were averaged to obtain one representative spectrum for each material. Each spectrum was normalized to the 1320 cm^{-1} band, cyclohexane C—C stretch, as this band was used for this aliphatic PU as the main reference peak.[27] Qualitative analysis was used to investigate the differences between spectra for the unimplanted and explanted samples. For those materials with polyether soft segments, attention was focused on the spectral regions corresponding to the carbonyl groups (non-hydrogen-bonded urethane carbonyl stretching at 1720 cm^{-1}), ether methylene (1365 cm^{-1}), and the ether groups (aliphatic asymmetric C—O—C stretch near 1110 cm^{-1} and aliphatic symmetric C—O—C stretch at 1080 cm^{-1}).[28–31] The appearance of 1174 cm^{-1} band was also checked, because this band was frequently observed in the degraded PEU, and was assigned to a branched ether created by crosslinking of the soft segments.[29]

Statistical analysis

Multiple samples were collected for each set of conditions ($n = 4$) and expressed as mean ± standard deviation (SD). Single factor analysis of variance (ANOVA) method was used to assess the statistical significance of the result. p values less than 0.05 were considered significant.

RESULTS

Optical micrographs of the explanted PU and nanocomposites are shown in Figure 1. The pure PU suffered from severe surface degradation, manifested as pits and cavities [Fig. 1(a)]. The degradation was reduced by addition of Au (17.4–65 ppm) or Ag (30.2–75.5 ppm) [Fig. 1(b–g)]. Among all nanocomposites, PU-Au 43.5 ppm and PU-Ag 30.2 ppm showed the least surface degradation [Fig. 1(c,e)].

Representative FESEM images at 1000× magnification for the explanted PU and nanocomposites are shown in Figure 2. The pure PU showed signs of deep aggressive cracks after implantation [Fig. 2(a)]. PU-Au 43.5 ppm and PU-Ag 30.2 ppm showed a relatively smooth surface [Fig. 2(c,e)] that changed little after implantation. However, pits and cracks again appeared frequently when Au increased to 65 ppm [Fig. 2(d)] and Ag increased to 75.5–113 pm [Fig. 2(f,g)].

Figure 3 shows the mean degradation ratings for PU and nanocomposites. The presence of Au or Ag nanoparticles in the nanocomposites at all contents reduced the surface degradation of PU. Especially, PU-Au 43.5 ppm and PU-Ag 30.2 ppm had the least surface degradation. The ranking of biostability based on less surface degradation was in the order of: PU-Ag 30.2 ppm ≈ PU-Au 43.5 ppm > PU-Ag 75.5 ppm > PU-Au 65 ppm > PU-Au 17.4 ppm > PU-Ag 113 ppm > pure PU.

The histological analysis of explanted PU and nanocomposites is illustrated in Figure 4. The pure PU showed significant infiltration of inflammatory cells [Fig. 4(a)]. PU-Au 43.5 ppm [Fig. 4(c)] and PU-Ag 30.2 ppm [Fig. 4(e)] showed intact boundary and little infiltration of inflammatory cells, that is they had very low foreign body reactions. Judging from the histology, the biocompatibility was ranked in the order of: PU-Ag 30.2 ppm ≈ PU-Au 43.5 ppm > PU-Ag 75.5 ppm > PU-Au 65 ppm > PU-Au 17.4 ppm > PU-Ag 113 ppm > pure PU. This was exactly the same order as that of biostability based on less surface degradation.

The chemical analysis of the polymer surface can indicate specific molecular alterations following implantation. Peak height analysis in the ATR-IR spectra was used to quantify the chemical changes of PU and nanocomposites after implantation. The peak at 1320 cm^{-1} in the samples, assigned to the cyclohexane C—C stretch, was used as the reference peak for this aliphatic PU. All spectra were normalized to this reference peak. Peak height analysis of the 1110 cm^{-1}

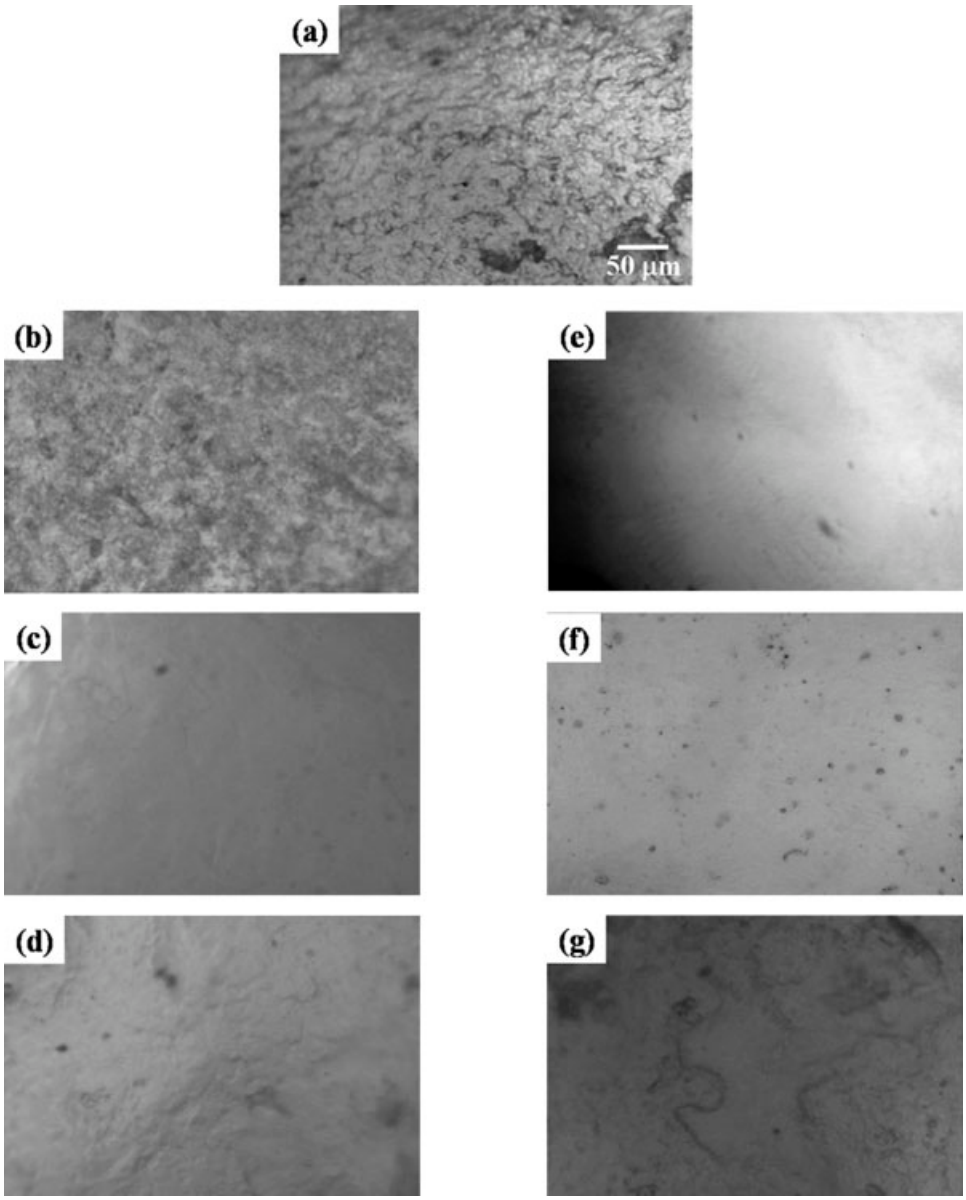

Figure 1. The surface degradation of implanted samples visualized by optical microcopy clearly presenting a less ruffling surface for PU-Au 43.5 ppm and PU-Ag 30.2 ppm. (a) pure PU; (b–d) the PU-Au nanocomposites at 17.4 ppm (b), 43.5 ppm (c), and 65 ppm (d) of Au; (e–g) PU-Ag nanocomposites at 30.2 ppm (e), 75.5 ppm (f), and 113 ppm (g) of Ag.

(ether), 1365 cm^{-1} (α-methylene), and 1720 cm^{-1} (non-H-bonded carbonyl) peaks for explanted PU and nanocomposites is shown in Figures 5–7. The apparent order of susceptibility to oxidation, as shown by the loss of 1110 cm^{-1}, was: pure PU ≈ PU-Ag 113 ppm > PU-Au 17.4 ppm > PU-Au 65 ppm > PU-Ag 75.5 ppm > PU-Au 43.5 ppm ≈ PU-Ag 30.2 ppm. Similar trends were seen with peak height analysis of ether methylene at 1365 cm^{-1} (except PU > PU-Ag 113 ppm) as well as non-hydrogen-bonded C=O at 1720 cm^{-1}.

Figure 8 illustrates the ATR-IR spectra in the region of 1300–1000 cm^{-1} for each sample before and after implantation. The pure PU after implantation had a significant loss at both the 1110 cm^{-1} soft segment ether peak and the 1080 cm^{-1} hard segment ether peak compared to the original before implantation [Fig. 8(a)]. The weak new peak at 1174 cm^{-1} was clearly observed. The explanted PU-Au 43.5 ppm [Fig. 8(c)] showed little change from the unimplanted specimen. Besides, there was no indication of the branched ether peak around 1174 cm^{-1}. Similar results were seen in the spectrum of the explanted PU-Ag 30.2 ppm [Fig. 8(e)], where little change from the unimplanted specimen was found. All the other nanocomposites showed the appearance of 1174 cm^{-1} and various degrees of change in the spectra after implantation.

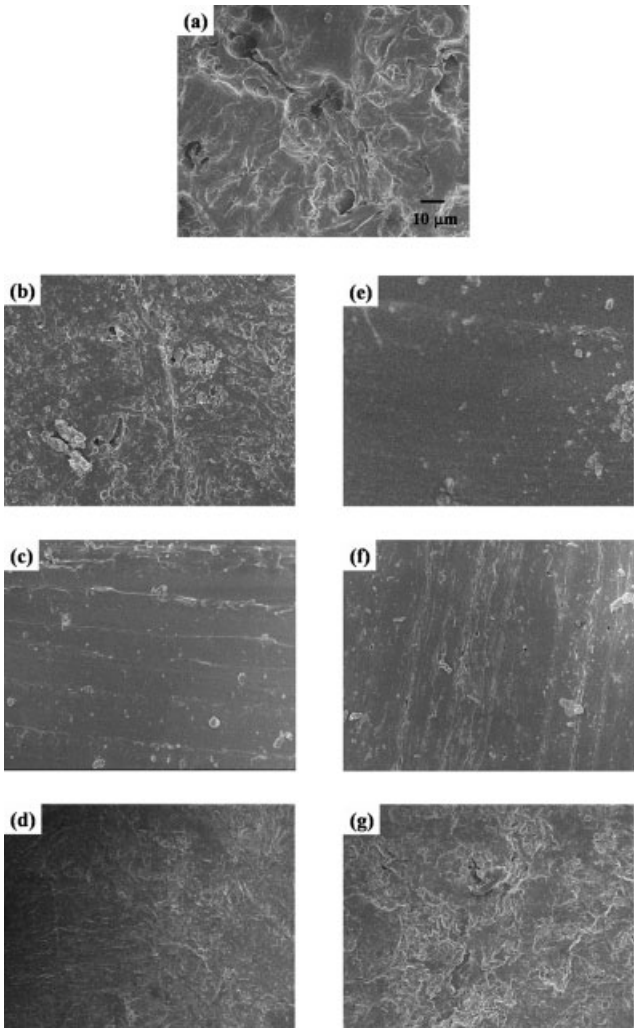

Figure 2. The surface degradation of implanted samples visualized by FESEM clearly presenting a less pitting/cracking surface for PU-Au 43.5 ppm and PU-Ag 30.2 ppm. (a) pure PU; (b–d) the PU-Au nanocomposites at 17.4 ppm (b), 43.5 ppm (c), and 65 ppm (d) of Au; (e–g): PU-Ag nanocomposites at 30.2 ppm (e), 75.5 ppm (f), and 113 ppm (g) of Ag.

DISCUSSION

From the optical micrographs and FESEM images, the pure PU clearly displayed the least resistance to degradation with most of the specimens fragmenting or undergoing deep, aggressive degradation. The pitting of surface was attributed to extraction of low-molecular-weight degradation products that resulted from chain scission.[32] The pit size decreased when Au or Ag was added. The nanocomposites PU-Au 43.5 ppm and PU-Ag 30.2 ppm had similar biostability with the majority of images free of signs of degradation. When the Au contents increased from 43.5 to 65 ppm, more surface degradation was observed. Similar situation also occurred when the Ag contents increased from 30.2 ppm to higher numbers. The ratings reflected these observations. As previously reported,[17–20] the amount of Au or Ag had a strong influence on the hydrogen-bonding formed, thermal and mechanical properties, hard domain size, and the free radical scavenging ability of the nanocomposites. The presence of a suitable amount of Au or Ag in the PU matrix stabilized the polymer chains and served to prevent oxidation. However, when the Au or Ag contents were beyond the proper range, the nanoparticles could form aggregates and cause the unfavorable changes. It has been reported that the addition of single-wall carbon nanotubes (SWNT) into poly(propylene fumarate) at low concentrations increased the rheological and mechanical properties but the effects decreased at higher concentrations because of aggregation of SWNT.[33] These observations suggested that the dispersion of nanomaterials be a critical factor to determine the final properties of the nanocomposites.

Analysis of the ATR-IR spectra for the explanted pure PU also revealed significant surface degradation. The chemical changes caused by biodegradation in porcine implants were consistent with severe oxidation of the aliphatic polyether soft segment and hydrolysis of the urethane bonds joining hard to soft segments. The decrease of the polyether soft-segment bands was attributed to oxidative attack on the soft-segment ether, resulting in chain scission. The appearance of the weak new peak at 1174 cm^{-1}, previously assigned to branched ether,[29] is thought to indicate that some crosslinking also occurred. Oxygen radicals abstract a proton from the α-methylene position of the polyether, resulting in chain scission or crosslinking of the PU.[29] In contrast, the spectrum of

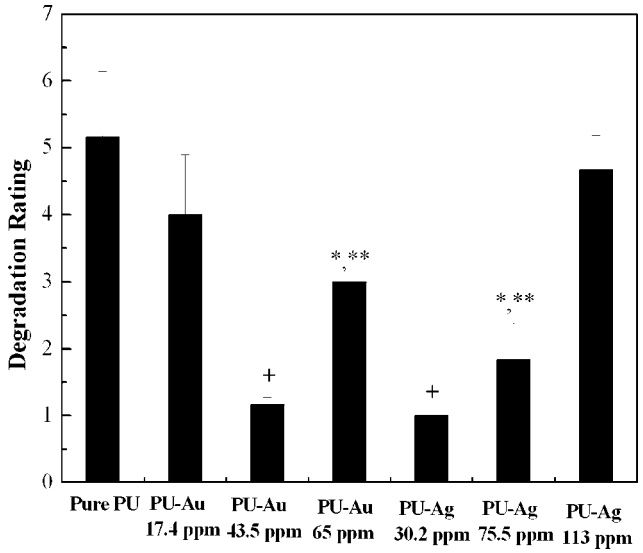

Figure 3. Degradation ratings for pure PU and nanocomposites after implantation. Significance ($p < 0.05$): *smaller than PU, **smaller than PU-Au 17.4 ppm and PU-Ag 113 ppm, $^{+}$small than all the other samples.

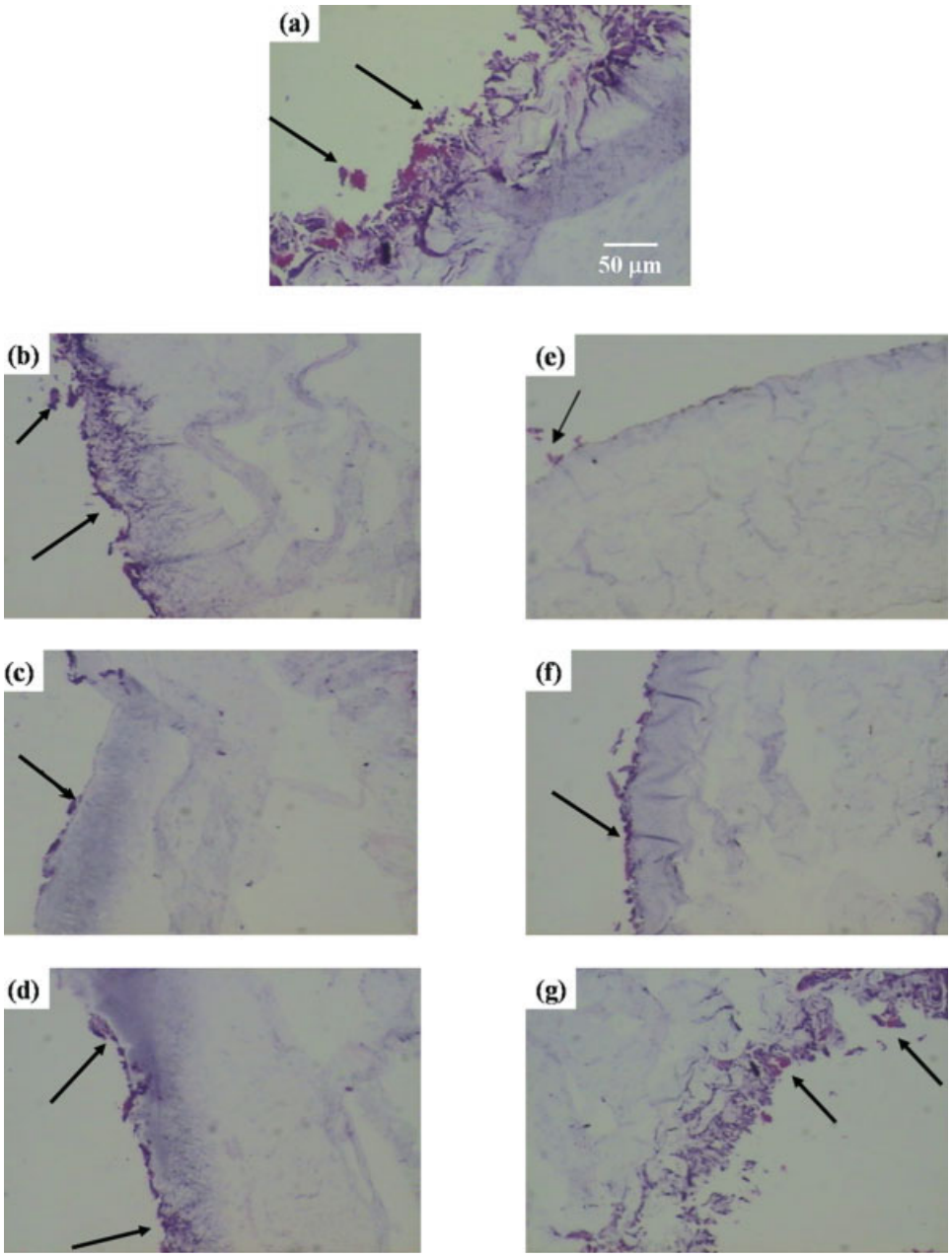

Figure 4. The histology of the implanted samples demonstrating much benign foreign body reactions of the PU-Ag nanocomposites (a) pure PU; (b–d) the PU-Au nanocomposites at 17.4 ppm (b), 43.5 ppm (c), and 65 ppm (d) of Au; (e–g) PU-Ag nanocomposites at 30.2 ppm (e), 75.5 ppm (f), and 113 ppm (g) of Ag. Arrows indicate the presence of inflammatory cells. [Color figure can be viewed in the online issue, which is available at www.interscience.wiley.com.]

the explanted PU-Au 43.5 ppm or PU-Ag 30.2 ppm remained very similar to that of the unimplanted specimen. The ranking order of biostability demonstrated in this study was in good accordance with the free radical scavenging ability of the series of PU nanocomposites reported earlier.[20] The main mechanism for biodegradation of PEU has been found to be oxidation.[7,29,30,34-36] Inhibition of cell-mediated biodegradation would be indicated by low cell adhesion, high levels of apoptosis, or conversion of macrophages to foam cells, a cell type unable to release oxygen radicals.[11] The α-carbon of the polyether soft segment of PEU is highly susceptible to oxidation by free radicals to form ester.[29] Therefore, the PU nanocomposites that were oxidatively stable had lower rates of degradation.

Histological analysis demonstrated the better biocompatibility of PU-Au and PU-Ag nanocomposites. The infiltration of inflammatory cells was significantly reduced, especially in PU-Au 43.5 ppm and PU-Ag 30.2 ppm. The biocompatibility of the series of PU nanocomposites in porcine models was accurately

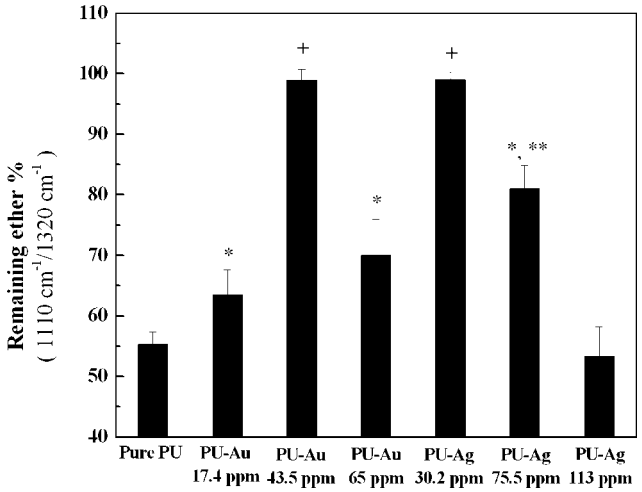

Figure 5. Surface associated biodegradation of the polyether soft segment after implantation by peak height analysis of the 1110 cm^{-1} ether linkage normalized to 1320 cm^{-1} reference peak. Significance ($p < 0.05$): *higher than PU, **higher than PU-Au 17.4 ppm and PU-Ag 113 ppm, $^{+}$higher than all the other samples.

reflected by their biostability. Schubert et al.[11] described that the biocompatibility depended not only on the properties of the polymer but also on its biostability. They hypothesized a cell-polymer feedback system for the control of biocompatibility and biostability of PU *in vivo*. A sequence of events is initiated by the implantation of the polymer. The wound initiates cell migration to the implant site. Polymer surface properties, protein adsorption, as well as the conformation and activity of the adsorbed proteins, thereby influenced the cell adhesion and activation. Adhered, activated cells then release free radicals during their respiratory burst and modify further cell migration and activity through mediator secretion, all of which lead to PU degradation. The products of this degradation can in turn influence cellular migration, adhesion and activation, and promote degradation autocatalytically. The distinct surface morphology and the free radical scavenging ability of the nanocomposites in this study may attract and activate less inflammatory cells.[20] At the same time, the nanocomposites are able to capture the free radicals produced by the inflammatory cells that may cause the degradation. The lower rates of degradation can reduce the degradation products, inhibit the subsequent release of such products and, through the feedback system as proposed by Schubert et al.[12] reduce the otherwise recruited cells and further inflammatory response.

It has been shown that the corrosion products from the metallic components from pacemaker lead wire coils were strong catalysts for PEU oxidation. *In vitro*, radicals can be initiated by metal ion/oxygen complex formation. *In vivo*, the macrophages and FBCGs on the PEU surface as part of the foreign body response also release hydrogen peroxide. This can permeate the polymer to react on the surface of the metal and produce oxygen free radicals inside the device in intimate contact with the PEU to facilitate autoxidation. Metal ions are released during this process, which can also react directly with the soft segment ether via redox reactions. These interactions have been called metal ion oxidation (MIO).[5,37,38] Contrary to the previous findings, in this study, the biostability of PEU was enhanced by the nanosize

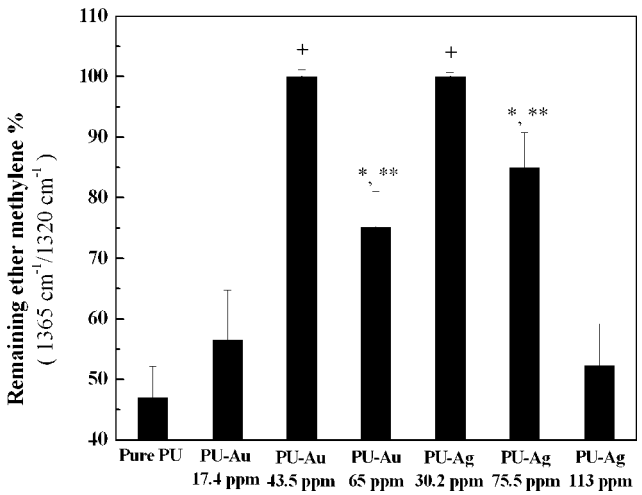

Figure 6. Surface associated biodegradation of the α-methylene after implantation by peak height analysis of the 1365 cm^{-1} ether linkage normalized to 1320 cm^{-1} reference peak. Significance ($p < 0.05$): *higher than PU, **higher than PU-Au 17.4 ppm and PU-Ag 113 ppm, $^{+}$higher than all the other samples.

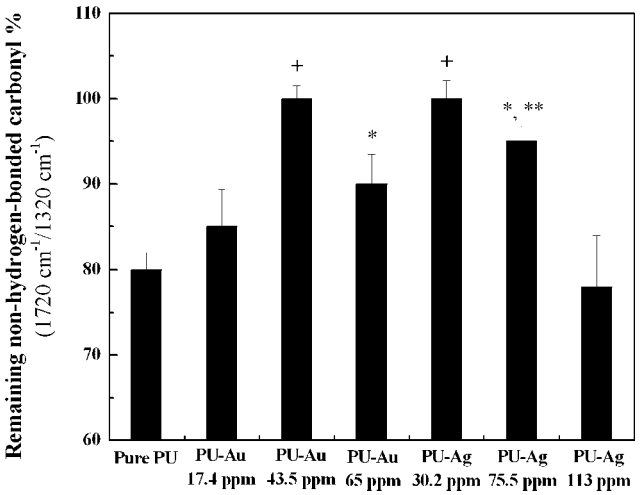

Figure 7. Surface associated biodegradation of the non-hydrogen-bonded urethane carbonyl after implantation by peak height analysis of the 1720 cm^{-1} normalized to 1320 cm^{-1} reference peak. Significance ($p < 0.05$): *higher than PU, **higher than PU-Au 17.4 ppm and PU-Ag 113 ppm, $^{+}$higher than all the other samples.

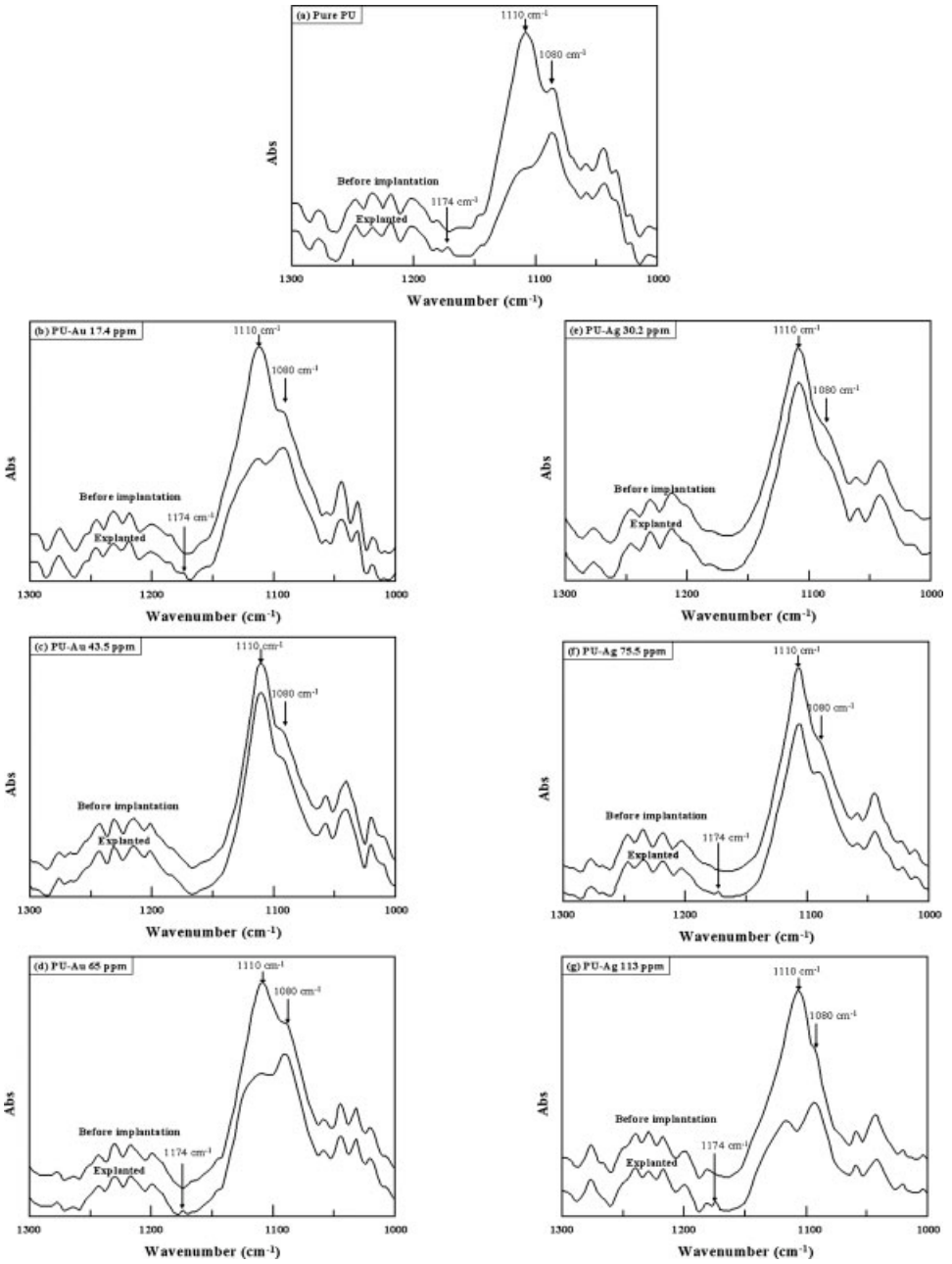

Figure 8. ATR-IR spectra showing some of the major changes between 1000 and 1300 cm^{-1} after implantation. (a) pure PU; (b–d) the PU-Au nanocomposites at 17.4 ppm (b), 43.5 ppm (c), and 65 ppm (d) of Au; (e–g) PU-Ag nanocomposites at 30.2 ppm (e), 75.5 ppm (f), and 113 ppm (g) of Ag.

metal particles (Au or Ag). Since the nanoparticles were added in PEU preparation, the morphology of the PEU has been significantly modified by the presence of nanoparticles. Furthermore, the PEU nanocomposites had greater free radical scavenging effect that was able to capture the free radicals produced by the inflammatory cells. This was a different mechanism from MIO.

The hypothesis for the much reduced biodegradation by addition of antioxidants such as vitamin E and Santowhite in solvent-borne PEU seemed to apply also to the waterborne PEU in this study.[11,12] More importantly, this study demonstrated a strong interdependency among antioxidation, biodegradation, and biocompatibility in the whole series of PU nanocomposites. As a matter of fact, the small amount of Au or Ag nanoparticles in PU nicely manipulated the range of their biological performance in porcine studies. The best performance was observed in PU-Au 43.5 ppm and PU-Ag 30.2 ppm. The associated chemical changes of these nanocomposites in the porcine model were parallel to those

reported for biodegradation/biostability of solvent-borne PEU in subcutaneous rats.[11,12,21,22] These nanocomposite systems served as a good model to further support the hypothesis of biocompatibility/biostability feedback system in PU.

CONCLUSION

The Au or Ag nanoparticles improved the biostability of waterborne PEU in porcine studies by inhibiting oxidation and crosslinking of the polyether soft segments. The improved biostability was most dramatically realized by PU-Au 43.5 ppm and PU-Ag 30.2 ppm that showed virtually no surface change after implantation. Increased biocompatibility was also demonstrated in PU-Au and PU-Ag nanocomposites, in good agreement with the improved biostability. The free radical scavenging ability of these nanocomposites could successfully predict their biostability and biocompatibility. The biocompatibility/biostability feedback hypothesis can be used to interpretate the biological performance of these PU nanocomposites in porcine models.

This work was conducted in the Center of Tissue Engineering and Stem Cells Research of this university. Gold nanoparticles were kindly supplied by Global Nanotech Industries Ltd. The corresponding author is jointly appointed by the Center of Nanoscience and Nanotechnology of the university.

References

1. Lamba N, Woodhouse K, Cooper S. Polyurethanes in biomedical applications. Boca Raton, FL: CRC press; 1998.
2. Hsu S, Tseng H, Wu M. Comparative in vitro evaluation of two different preparations of small diameter polyurethane vascular grafts. Artif Organs 2000;24:119–128.
3. Kuan H, Ma M, Chang W, Yuen S, Wu H, Lee T. Synthesis, thermal, mechanical and rheological properties of multiwall carbon nanotube/waterborne polyurethane nanocomposite. Compos Sci Technol 2005;65:1703–1710.
4. Kim B, Lee J. Waterborne polyurethanes and theirproperties. J Polym Sci Part A: Polym Chem 1996;34:1095–1104.
5. Stokes K, Coury A, Urbanski P. Autooxidative degradation of implanted polyether polyurethane devices. J Biomater Appl 1987;1:411–448.
6. Wiggins M, Wilkoff B, Anderson J, Hiltner A. Biodegradation of polyether polyurethane inner insulation in bipolar pacemaker leads. J Biomed Mater Res 2001;58:302–307.
7. Zhao Q, Topham N, Anderson J, Hiltner A, Lodoen G, Payet C. Foreign-body giant cells and polyurethane biostability: In vivo correlation of cell adhesion and surface cracking. J Biomed Mater Res 1991;25:177–183.
8. Stokes K, McVenes R. Polyurethane elastomer biostability. J Biomater Appl 1995;9:321–354.
9. Hsu S, Lin Z. Biocompatibility and biostability of a series of poly(carbonate)urethanes. Colloids Surf B 2004;36:1–12.
10. Christenson E, Wiggins M, Anderson J, Hiltner A. Surface modification of poly(ether urethane urea) with modified dehydroepiandrosterone for improved in vivo biostability. J Biomed Mater Res 2005;73:108–115.
11. Schubert M, Wiggins M, DeFife K, Hiltner A, Anderson J. Vitamin E as an antioxidant for poly(etherurethane urea) in vivo studies. J Biomed Mater Res 1996;32:493–504.
12. Schubert M, Wiggins M, Anderson J, Hiltner A. Comparison of two antioxidants for poly(etherurethane urea) in an accelerated in vitro biodegradation system. J Biomed Mater Res 1997;34:493–505.
13. Schon G, Simon U. A fascinating new field in colloid science: Small ligand-stabilized metal clusters and possible application in microelectronics. Colloid Polym Sci 1995;273:101–117.
14. Ramos J, Millán A, Palacio F. Production of magnetic nanoparticles in a polyvinylpyridine matrix. Polymer 2000;41: 8461–8464.
15. Zhang J, Wang B, Ju X, Liu T, Hu T. New observations on the optical properties of PPV/TiO_2 nanocomposites. Polymer 2001;42:3697–3702.
16. Chiang P, Whang W. The synthesis and morphology characteristic study of BAO-ODPA polyimide/TiO_2 nano hybrid films. Polymer 2003;44:2249–2254.
17. Hsu S, Chou C, Tseng S. Enhanced thermal and mechanical properties in polyurethane/Au nanocomposites. Macromol Mater Eng 2004;289:1096–1101.
18. Hsu S, Chou C. Enhanced biostability of polyurethane containing gold nanoparticles. Polym Degrad Stab 2004;85:675–680.
19. Chou C, Hsu S, Chang H, Tseng S, Lin H. Enhanced thermal and mechanical properties and biostability of polyurethane containing silver nanoparticles Polym Degrad Stab 2006;91: 1017–1024.
20. Hsu S, Tang C, Tseng H. Biocompatibility of poly(ether) urethane-gold nanocomposites. J Biomed Mater Res A 2006; 79:759–770.
21. Collier T, Tan J, Shive M, Hasan S, Hiltner A, Anderson J. Biocompatibility of poly(etherurethane urea) containing dehydroepiandrosterone. J Biomed Mater Res 1998;41:192–201.
22. Kao W, Hiltner A, Anderson J, Lodoen G. Theoretical analysis of in vivo macrophage adhesion and foreign body giant cell formation on strained poly (etherurethane urea) elastomers. J Biomed Mater Res 1994;2:819–829.
23. David D, Staley H. Analytical chemistry of the polyurethane. New York: Wiley-Interscience; 1969. p 357–359.
24. Hsu S, Chen J. Enhanced biostability by using butenediol as chain extenders in the synthesis of poly(ether)urethanes. Polym Degrad Stab 1999;65:341–345.
25. Hergenrother RW, Wabers HD, Cooper SL. Effect of hard segment chemistry and strain on the stability of polyurethanes: In vivo biostability Biomaterials 1993;14:449–458.
26. Hsu S, Huang T. The susceptibility of poly(ether)urethanes to enzymatic degradation after oxidative pretreatment. Polym Degrad Stab 2000;67:171–178.
27. McCarthy S, Meijs G, Mitchell N, Gunatillake P, Heath G, Brandwood A, Schindhelm K. In-vivo degradation of polyurethanes: Transmission-FTIR microscopic characterization of olyurethanes sectioned by cryomicrotomy. Biomaterials 1997;18: 1387–409.
28. Chen K, Kuo J, Chen C. Synthesis, characterization and platelet adhesion studies of novel ion-containing aliphatic polyurethanes. Biomaterials 2000;21:161–171.
29. Schubert M, Wiggins M, Schaefer M, Hiltner A, Anderson J. Oxidative biodegradation mechanisms of biaxially strained poly(etherurethane urea) elastomers. J Biomed Mater Res 1995;29:337–347.
30. Wu Y, Sellitti C, Anderson J, Hiltner A, Lodoen G, Payet C. An FTIR-ATR investigation of in vivo poly(etherurethane) degradation. J Appl Polym Sci 1992;46:201–211.

31. Mathur A, Collier T, Kao W, Wiggins M, Schubert M, Hiltner A, Anderson J. In vivo biocompatibility and biostability of modified polyurethanes. J Biomed Mater Res 1997;36:246–257.
32. Renier M, Wu Y, Anderson J, Hiltner A, Lodoen G, Payet C. Characterization of extractable species from poly(etherurethane urea) (PEUU) elastomers. J Biomed Mater Res 1994;5:511–529.
33. Shi X, Hudson J, Spicer P, Tour J, Krishnamoorti R, Mikos A. Rheological behaviour and mechanical characterization of injectable poly(propylene fumarate)/single-walled carbon nanotube composites for bone tissue engineering. Nanotechnology 2005;16:S531–S538.
34. Wu Y, Zhao Q, Anderson J, Hiltner A, Lodoen G, Payet C. Effect of some additives on the biostability of a poly(etherurethane) elastomer. J Biomed Mater Res 1991;25:725–739.
35. Zhao Q, Anderson J, Hiltner A, Lodoen G, Payet C. Theoretical analysis on cell size distribution and kinetics of foreign-body giant cell formation in vivo on polyurethane elastomers. J Biomed Mater Res 1992;26:1019–1038.
36. Anderson J, Hiltner A, Zhao Q, Wu Y, Renier M, Schubert M, Brunstedt M, Lodoen G, Payet C. Cell/polymer interactions in biodegradation of polyurethanes. In: Vert M, editor. Biodegradable Polymers and Plastics. Cambridge: Royal Society of Chemistry; 1992. p 122–136.
37. Takahara A, Coury AJ, Hergenrother RW, Cooper SL. Effect of soft segment chemistry on the biostability of segmented polyurethanes. I. In vitro oxidation. J Biomed Mater Res 1991;25:341–356.
38. Ward R, Anderson J, McVenes R, Stokes K. In vivo biostability of polyether polyurethanes with fluoropolymer and polyethylene oxide surface modifying endgroups; resistance to metal ion oxidation. J Biomed Mater Res A 2007;80:34–44.